Article

Modified 3D Ewald Summation for Slab Geometry at Constant Potential

Matheus Girotto* and Adriano Mesquita Alencar

Read Online

ACCESS | Metrics & More | Article Recommendations

ABSTRACT: We present a new Monte Carlo method to simulate ionic liquids in slab geometry at constant potential. The algorithm is built upon two previous methods while retaining the advantages of each of them. The method is tested against a Poisson–Boltzmann theory and the constant surface charge ensemble, achieving consistency among all of them. We then analyze the computational time of the developed algorithm, showing substantial speedup in relation to the method of Kiyohara and Asaka [*J. Chem. Phys.*, **2007**, *126*, 214704]. As an application of our method, we investigate crowding and overscreening in confined room-temperature ionic liquids. We show that we can switch between two behaviors of the double layer by changing the Bjerrum length alone.
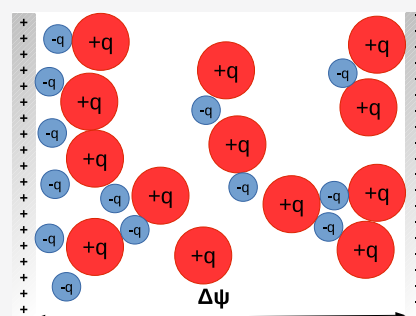
I. INTRODUCTION

Since the appearance of computing machines, Ewald summation is a ubiquitous algorithm in physical chemistry. This is because many systems of scientific interest have components with bare electric charge at the atomic scale: nanoconfined electrolytes,[1−4] polyelectrolytes near flat surfaces,[5,6] ionic liquid supercapacitors,[7−11] and electrolyte-based electrowetting devices[12,13] are just a handful of examples. The proper computational simulation of these systems requires Ewald summation techniques to calculate the energy of the target system.[14] In this article, we present a new method to efficiently simulate confined charged liquids at constant potential, using a modified three-dimensional (3D) Ewald summation and a Monte Carlo (MC) algorithm. The system is illustrated in Figure 1.

The calculation of bulk electrostatic energies has its beginning in 1921 when the German physicist Paul Peter Ewald set out to calculate the energy of cubic-lattice crystals.[15]

Figure 1. Illustration of the system in a two-dimensional projection.

Considering the distance between cations and anions a, the so-called lattice constant, q the proton charge, and ϵ the permittivity of space, the electrostatic potential at one atom in the infinite system is

$$\phi = \sum_{i,j,k} (-1)^{i+j+k} \frac{q}{\epsilon a} \frac{1}{\sqrt{i^2 + j^2 + k^2}} = \frac{|e|}{\epsilon a} M \tag{1}$$

where $(i, j, k) \in \mathbb{Z}$, M is defined as the Madelung constant, and the technique used to evaluate the series is nowadays called Ewald summation. The summation excludes all indices equal to zero, and the $(-1)^{i+j+k}$ takes care of whether it is an anion or a cation, for example, the alternating atoms of sodium chloride. The basic idea of the method is to split the potential into a long- and a short-range contribution, computing the former on the reciprocal space and the latter on the real space.

Ewald summation is necessary because the Coulomb potential is long-ranged, which means it extends to infinity. Therefore, simple nearest neighbors periodic boundary conditions of the main box, as used in short-ranged potentials, are not enough. One has to consider infinite replicas of the main simulation cell to achieve the thermodynamic equilibrium. These series of replications are tackled with Ewald's method and its many optimizations realized over the years.[16−21] Unfortunately, Ewald summation methods are
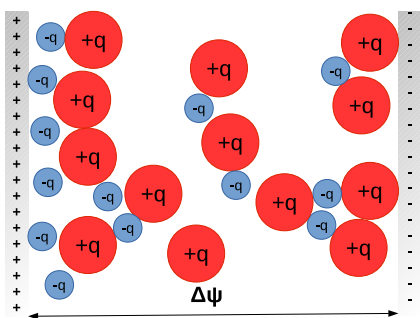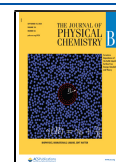
efficient when the system is isotropic, i.e., it has periodicity in three dimensions. When one dimension is finite, much of the velocity of the convergence is lost, since the Fourier transformation of the long-range potential yields special functions in a slowly convergent series.[22,23] However, this geometry is present in electrolytes or ionic liquids confined by capacitor plates and many more systems of intense technological interest.[24−30] Therefore, optimizations were devised to overcome this computational time problem and to simulate these interesting systems in two-dimensional (2D) geometry.[31−35] The most successful one is by Yeh and Berkowitz (YB),[36] where the fast convergence is retained using an extra energy term and a vacuum region between the spurious replicas.

Following this tradition of optimizations, in this article, we present a new method that is able to rapidly simulate confined charged systems at constant potential. The method simulates a nano-supercapacitor; see Figure 1. The basic idea of the article is to merge the method by Levin et al.[37] with the method by Kiyohara and Asaka (KA),[38] retaining the positive points of both. While the method by Levin et al. is applied to the constant charge ensemble, we adapt it for the ensemble proposed by KA. With our new algorithm, we avoid special functions used by KA and have fast convergence, while still treating the charged plates as an external potential. At this very point lies the superiority in the velocity of our numerical trick.

After the derivation of the system's energy, we test the method against a mean-field Poisson−Boltzmann (PB) theory in the weak coupling limit and also against the constant surface charge ensemble, which is complementary in thermodynamics to the constant potential ensemble. All MC simulations and the PB theory agree, thus validating our algorithm. We then present a comparison of computational speeds between our developed method and the one by KA, which is basically a Lekner summation. Finally, we apply the method to study crowding and overscreening in confined ionic liquids. Computational speed is a cornerstone here, since ionic liquids have much higher volume fractions and ionic coupling than usual electrolytes. Furthermore, conclusions and guidelines for future work are presented at the end.

II. METHOD

Consider N charges q_j, with $j = (1, 2, ..., N)$, randomly positioned in the main simulation cell, with position vectors r_j. We replicate the simulation box of dimensions $L = (L_x, L_y, L_z)$ in every direction and define the charge densities $\rho_j(r_j) = q_j\delta(s - r_j - r_{rep})$, where $\delta(x)$ is the Dirac delta function, $r_{rep} = L\cdot n$ and $n = (n_x, n_y, n_z)$, where n_i's are integers. Thus, we can write an analogous equation of eq 1 in an integral form

$$\phi(r) = \sum_n \sum_{j=1}^N \int_V \frac{\rho_j(s)}{\epsilon|r-s|}ds \tag{2}$$

to calculate the electrostatic potential at an arbitrary position r of the simulation box. The integration is over all space and the replication vector r_{rep} projects the real charges in the replicated boxes, forming an infinite periodic system. The main box is at $n = (0, 0, 0)$. The core idea is now to split the potential into a long- and a short-range contribution. Thus, we perform a simple addition and subtraction of a function to the total potential, and then we write the potential as

$$\phi(r) = \sum_n \sum_{j=1}^N \int_V \frac{\rho_j(s) - \rho_{j,G}(s)}{\epsilon|r-s|}ds$$
$$+ \sum_n \sum_{j=1}^N \int_V \frac{\rho_{j,G}(s)}{\epsilon|r-s|}ds \tag{3}$$

where

$$\rho_{j,G}(s) = \frac{\kappa^3 q_j}{\sqrt{\pi^3}} \exp[\kappa^2|s-r_j - r_{rep}|^2] \tag{4}$$

Note that κ is an artificial, damping parameter and the total energy cannot depend on it for neutral systems. Other damping functions may be chosen. However, for speed purposes, this is a default choice. The terms of the right-hand side of eq 3 are the long- and short-range potentials. To compute the former, we perform a 3D Fourier transformation. This procedure is chosen to avoid 2D Fourier operators, from which complicated functions arise. We then take the limit from bulk to slab geometry to yield the correct potential. The short- and the long-range potentials assume the forms

$$\phi_{sr}(r) = \sum_{j=1}^N q_j \frac{\text{erfc}(\kappa|r-r_j|)}{\epsilon|r-r_j|}$$

$$\phi_{lr}(r) = \frac{4\pi}{\epsilon V} \sum_{k=-\infty}^{\infty} \sum_{j=1}^N \frac{q_j}{|k|^2} \exp[-\frac{|k|^2}{4\kappa^2} + ik\cdot(r - r_j)]$$

with $\phi(r) = \phi_{sr}(r) + \phi_{lr}(r)$
$$\tag{5}$$

The Fourier vectors are $k = (2\pi n_x/L_d, 2\pi n_y/L_d, 2\pi n_z/L_z)$, $V = L_d^2 L_z$ is the volume, and we set $L_x = L_y = L_d$, without any loss of generality. For the short-range potential, we consider just nearest neighbors periodic boundary conditions, excluding the sum over n. This is justified since the erfc(x) function decays exponentially fast with x.

We note that the term corresponding to $k = 0$ diverges in the long-range potential, ϕ_{lr}. This divergence has a long debate recorded in the literature; see for example refs 14, 39, 40, where it is discussed how to properly handle the infinite term. In the present work, we are interested in slab geometry, while retaining the speed of 3D Ewald summation, where the system of interest is isotropic in three directions. To achieve this, we follow the study by Levin and co-workers,[37] where a detailed treatment of the term $k = 0$ is performed for slab geometry. There the $\vec{k} = (0, 0, 0)$ divergence gives rise to an energy term that is dependent solely on the geometry of the system. That is, even for isotropic systems, the contribution exists and it is usually neglected. In the paper, they explain that this omission usually does not affect isotropic systems on average. Most importantly, they deduce the term for slab geometry rigorously. Levin's method was inspired by the YB algorithm. The main difference is that it does not appeal to the so-called tinfoil boundary at infinity, for there is no sense in an infinitely replicated system to be bounded. The energy term, which is due to specific periodic boundary conditions, was derived using rigorous methods to sum over conditionally convergent series. Therefore, as shown in ref 37, for slab-shaped systems, the term arises due to the summation infinitely faster in the periodic directions in comparison with the sum in the nonperiodic dimension. Moreover, a vacuum region must be
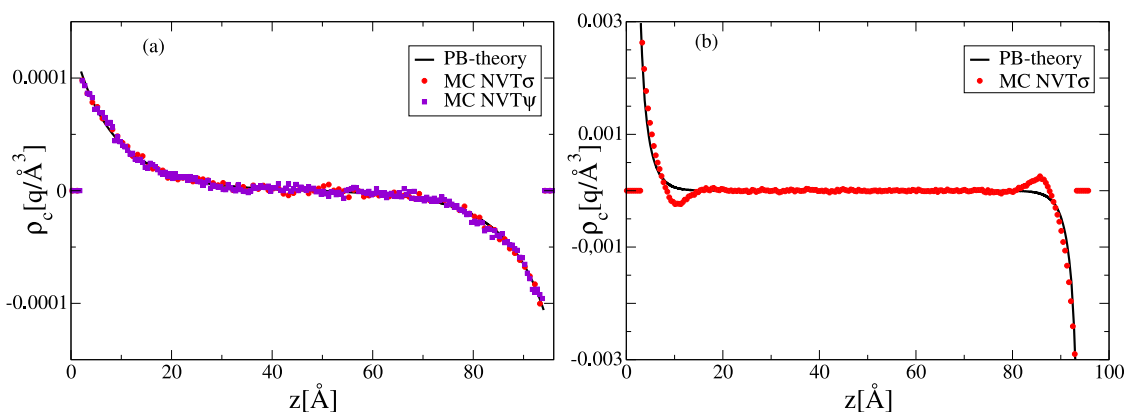
Figure 2. Charge densities ρ_c for a 1:1 and a 2:2 electrolyte in panels (a) and (b), respectively. (a) Mutual consistency of all approaches, thus validating the new algorithm. The parameters are $\sigma = 0.015$ C/m^2, $\rho = 100$ mM, and radius of particles $R = 2$ Å. These parameters represent the weak coupling limit. (b) In the strong coupling limit, where higher charge densities and bigger molar concentrations are present, the mean-field approach is doomed to fail, as shown. The parameters are $\rho = 550$ mM, $\sigma = 0.075$ C/m^2, and $R = 3$ Å. The distance between the plates is $L = 96$ Å.

inserted between the slabs to nullify the effects of the undesired replicas in the z dimension. This is due to the fact that we still perform a "slow" summation in z. In addition, the algorithm allows one to consider the charged slabs as an external potential, this way avoiding the construction of the plates with point charges. This slow procedure to construct the confinement basically spreads equally separated point charges in the plane and adjusts the Coulomb charge to match the desired surface density. Its slowness is due to the fact that at each simulation step the points must be considered in the main loop of the simulation. Thus, we note that the modified Ewald summation by Levin et al. suits perfectly to be merged with the algorithm by KA, since then the plates are also treated as an external potential. The main disadvantage of the KA algorithm is the appearance of Bessel functions in the ion–ion interaction, which we overcome in the present new method using only exponentials, resulting in a much faster convergent series.

Following eq 6 and Levin, Girotto, and dos Santos,[37] we write the potentials of the now confined ions. The confinement appears due to the summation mentioned above, i.e., due to the specific treatment of the divergent term $|k| = 0$. The ion–ion (i–i) potential and the ion–plate (i–p) potential are thus written

$$\phi_{i-i}(r) = \frac{4\pi}{\epsilon V} \sum_{k \neq 0}^{\infty} \sum_{j=1}^{N} \frac{q_j}{|k|^2} \exp[-\frac{|k|^2}{4\kappa^2} + ik \cdot (r - r_j)]$$
$$+ \sum_{j=1}^{N} q_j \frac{\text{erfc}(\kappa|r - r_j|)}{\epsilon|r - r_j|} - \frac{2\pi}{\epsilon V} \sum_{j=1}^{N} q_j (z - z_j)^2$$

$$\phi_{i-p}(z) = \frac{4\pi\sigma}{\epsilon} \sum_{j=1}^{N} z_j$$

(6)

where σ is the charge density of the plates and $\phi(r) = \phi_{i-i}(r) + \phi_{i-p}(z)$. The third term to the right of ϕ_{i-i} is the contribution to the energy that arises precisely from the consideration of the confinement of the ions. However, for the following constant potential partition function of the KA ensemble

$$\mathcal{Z}_\psi = \int \prod_{j=1}^{N} dr_j \int d\sigma \, \exp\left\{ \frac{-1}{k_B T} [U(r_1, ..., r_N, \sigma) \right.$$
$$\left. - \psi\sigma L_d^2] \right\}$$

(7)

where ψ is the external potential applied to the cell, we also need the interaction of the plates with each other. This way we properly consider the dependence of the total energy on the charge of the plates. The potential one plate produces in the other (p–p) is

$$\phi_{p-p} = \frac{2\pi\sigma}{\epsilon} L$$

(8)

where L is the distance between the plates. We note that the KA ensemble is complementary to the constant charge ensemble, $NVT\sigma$, and for our algorithm to be valid, it must obey the equivalence of ensembles, as shown in Figure 2a. To obtain the proper total energy, $U(r_1, ..., r_N, \sigma)$, we double sum over the potentials, considering now the plate–plate (p–p), plate–ion, and ion–ion interactions

$$U(r_1, ..., r_N, \sigma) = \frac{1}{2} \sum_{j \neq i} q_i \phi(r_i) + \frac{2\pi\sigma^2}{\epsilon} L_d^2 L$$
$$= U_{i-i} + U_{i-p} + U_{p-p}$$

(9)

where the second term on the first equality is the plate–plate energy. $U_{i-p} + U_{p-p}$ yields all energies that are not interionic. We write them separately due to the fact that the difference in energies between the present algorithm and the one used by KA is only the ion–ion energy. Therefore, by simply replacing the decoupled energy, one can update the KA-based code to a faster version. This is one of the main advantages of our method. The interionic energy is

$$U_{i-i} = \frac{2\pi}{\epsilon V} \sum_{k \neq 0} \frac{|S(k)|^2}{|k|^2} e^{-|k|^2/4\kappa} + \frac{1}{2} \sum_{j \neq i} q_i q_j \frac{\text{erfc}(\kappa|r_i - r_j|)}{\epsilon|r_i - r_j|}$$
$$+ \frac{2\pi}{\epsilon V} \left(\sum_i q_i z_i \right)^2 - \frac{\kappa}{\epsilon\sqrt{\pi}} \sum_i q_i^2$$

(10)

with $S(\mathbf{k}) = \sum_i q_i \exp(\mathbf{k} \cdot \mathbf{r}_i)$ and the last term to the right is the so-called self-energy. The remaining energy is due to the plate−ion interaction and plate−plate interaction, defined as

$$U_{\text{i}-\text{p}} + U_{\text{p}-\text{p}} = \frac{4\pi\sigma}{\epsilon} \sum_i q_i z_i + \frac{2\pi}{\epsilon} L \sigma^2 L_d^2 \tag{11}$$

We note that for the constant charge ensemble the plate−plate interaction is constant, and then it may be set to zero, and $\psi = 0$. This way one can recover the canonical ensemble from eq 7, resulting in the ensemble used in Levin's paper. Finally, the ion−ion interaction in the paper by KA is

$$U_{\text{i}-\text{i},\text{KA}} = 2 \sum_{i \neq j} \frac{q_i q_j}{\epsilon L_d} \sum_{n=1}^{\infty} \sum_{m=-\infty}^{\infty} \cos\left(\frac{2\pi n}{L_d} x_{ij}\right) K_0\left[2\pi n \sqrt{\left(\frac{y_{ij}}{L_d} + m\right)^2 + \left(\frac{z_{ij}}{L_d}\right)^2}\right]$$
$$- \frac{1}{2} \sum_{i \neq j} \frac{q_i q_j}{\epsilon L_d} \ln\left[\cosh\left(\frac{2\pi}{L_d} z_{ij}\right) - \cos\left(\frac{2\pi}{L_d} y_{ij}\right)\right] - \sum_{i \neq j} \frac{q_i q_j}{\epsilon L_d} \ln(\sqrt{2}) + U_s \tag{12}$$

where $(x_i - x_j, y_i - y_j, z_i - z_j) = (x_{ij}, y_{ij}, z_{ij})$ and U_s is a constant term that accounts for the self-energy and does not depend on positions. We point to the simplicity of eq 10 in comparison with eq 12, which will be reflected in computation speed. The extension of the methods to molecular dynamics simulations could be achieved by calculating the force on ion i with $\nabla_i U(\mathbf{r}_1,..., \mathbf{r}_N, \sigma) = \overrightarrow{F_i}$. However, this would increase the computational time of our algorithm, which is expected for molecular dynamics simulations when compared to Monte Carlo.

III. POISSON−BOLTZMANN THEORY

Using the first Maxwell equation

$$\nabla \cdot \mathbf{E}(\mathbf{r}) = \frac{4\pi}{\epsilon} \rho(\mathbf{r}) \tag{13}$$

and the PB theory, we can consider the distribution of charges in a first approximation as "smeared" over a constant dielectric background. The PB theory is ubiquitous in liquid theory and successfully explains a range of physical and chemical phenomena.[41] It is, more generally, a nonlinear version of the Debye−Hückel theory, first proposed in the beginning of the last century to explain the osmotic pressure of dilute electrolytes. Furthermore, in the PB theory, the density distribution is governed by the Boltzmann−Gibbs statistics and is an approximation to the level we can ignore charge−charge positional correlations and consider a mean-field electric potential. Hence, it is valid for weakly interacting liquids, contrary to the case of room-temperature ionic liquids, even if artificial steric effects are introduced.[42−44] Thus, for an electrolyte in slab geometry, we write

$$-\nabla^2 \phi(z) = \frac{4\pi}{\epsilon}\left[\sum_{i=+,-} \frac{1}{L_d^2} \frac{N_i q_i e^{-\beta q_i \phi(z)}}{\int_0^d e^{-\beta q_i \phi(z')} dz'} - \sigma\delta(z) + \sigma\delta(z-L)\right] \tag{14}$$

where N_+ is the number of anions and N_- is the number of cations. q_+ and q_- are their charges, respectively. The first term is the distributed charge in accordance with the Boltzmann weights and the Dirac deltas are the charges of the plates, positioned at $z = 0$ and $z = L$. To solve this equation, we integrate over volume, apply the divergence theorem on the electric field, and obtain

$$E(z) = \frac{4\pi}{\epsilon} \int_0^z dz' \left[\sum_{i=+,-} \frac{1}{L_d^2} \frac{N_i q_i e^{-\beta q_i \phi(z')}}{\int_0^d e^{-\beta q_i \phi(z')} dz'} - \sigma\delta(z') + \sigma\delta(z' - L)\right] \tag{15}$$

with β the inverse thermal energy. With the relation $E(z) = -\int_0^z \phi(z') dz'$, we can solve eqs 14 and 15 iteratively using the Picard iteration. We begin with an initial guess to the potential and a mixing parameter of $\gamma = 0.95$. The latter parameter is artificial, and it is used to improve the range of convergence of the theory. It must be found by trial and error to optimize the computational time and the temperature/density scope of the theory.

IV. VALIDATION OF ALGORITHM

We begin performing MC simulations at the constant potential ensemble, $NVT\psi$, and at the constant surface charge ensemble, $NVT\sigma$. We first let the $NVT\sigma$ ensemble simulation relax to equilibrium and extract the averaged electric potential difference between the plates

$$\phi(z) = -\frac{4\pi}{\epsilon} \int_0^z dz' \int_0^{z'} \rho_c(z'') dz''$$
$$= -\frac{4\pi}{\epsilon} \int_0^z dz' \rho_c(z')((z-z') \tag{16}$$

where ρ_c is the charge density and $\psi = \phi(L)$ will be used as input to the MC algorithm at the $NVT\psi$ ensemble. The equivalence of ensembles is the first trial of our new method.

The simulations through this work are performed with the Metropolis algorithm, using 10^6 steps to achieve the thermodynamic equilibrium and using 5×10^4 uncorrelated samples to extract the averaged system properties. We use long- and short-range movements to properly and efficiently sample the phase space. The long-range movements are trial displacements that assign a new random position to the chosen particle in the whole box, helping the system avoid local free energy minima. The proportion is 1:10 in relation to short-range movements, in which the particle moves only a random fraction of its radius. Considering the $NVT\psi$ ensemble, we must perform one type of trial movement that is a transfer of a random amount of charge from one plate to another. This is done to the average charges on the plates achieve the equilibrium state. Again, the proportion is 1:10 in relation to the trial movements related to the spatial displacements of particles. We adjust the maximum of charge exchanged on the fly, to make sure 1/2 of the trials are accepted. We use 1377 $\mathbf{k}$-vectors to compute the long-range energy, summing 2 times more vectors in the k_z direction in relation to remaining dimensions. Thus, we set the vacuum region $L_{\text{vac}} = L$, which is enough to avoid interactions with the artificial replicas in the z dimension. The periodic dimensions $L_d = L_x = L_y$ are set to 96 Å. The distance L between the plates is chosen to guarantee a bulk-like regime in the electrolyte far away from each plate. The particles through the work are modeled as hardcore spheres with varying sizes. This is known as the primitive model of electrolytes. The Bjerrum length is defined as $\lambda_B = \beta q^2/\epsilon$, and it measures the strength of system interactions in relation to temperature, i.e., the distance at which the entropy energy is equal to electric potential energy. We test different initial conditions to ensure that no trap in free energy results in spurious data. This last point is unfortunately usually ignored in the literature and it is essential to ionic liquids, since the
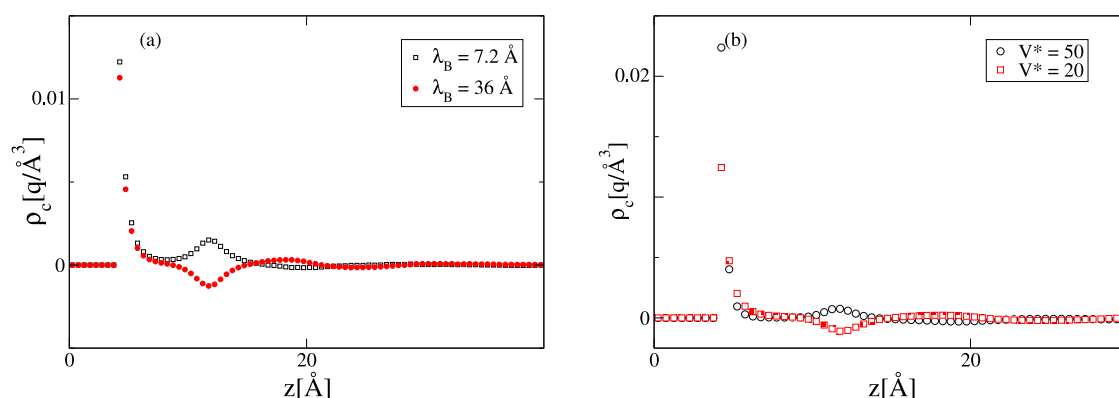
Figure 3. Charge densities ρ_c for 1:1 room-temperature ionic liquids: (a) Behavior of the double layer can be tuned between overscreening and crowding by the Bjerrum length alone, at constant potential $\psi = 20\ k_BT/q$. The Bjerrum lengths are indicated in the figure. (b) We simply show that the behavior can be tuned also by the applied voltage, as shown by Kornyshev and co-workers. The potentials are indicated on the plot, where $V^* = q\beta V$ and $\lambda_B = 36$ Å, which is characteristic of ionic liquids at room temperature.

strong interactions form many local minima in the free energy landscape.

For analyzing the PB theory against MC simulations we set $\lambda_B = 7.2$ Å, which is characteristic of aqueous electrolytes. In Figure 2a, we show the equivalence of ensembles and consistency of our simulations with the PB theory, forming this way a solid stand to our algorithm. In Figure 2b, we show that the PB theory fails when the coupling strength of the system is high and when there are large densities and strong surface charges. We plot this figure to show that the mean-field approach will be inadequate to describe room-temperature ionic liquids, which have much higher volume fractions and Bjerrum lengths than weak electrolytes.[7] This gives rise to the necessity of computer simulations or to complicated liquid theoretical approaches, like density functional theory or integral equations. The authors further suggest that new approaches to liquid theory that rely on solid statistical mechanical grounds are necessary to overcome the challenge of properly describing ionic liquids theoretically.

V. IONIC LIQUIDS AND COMPUTATIONAL TIME

We use both eqs 12 and 10 to compare computational times, calculating the initial energy of a system of 1000 randomly positioned particles. We prepare 1000 initial states and measure the average computational time to perform the energy calculations. The parameters of the Ewald summation are the same as in previous sections, while for the Lekner summation, we used $35n$ replicas and $11k$ replicas. These numbers are typical of Lekner summation. Our algorithm performed 2 orders of magnitude faster than the one by KA. More specifically, for this number of particles, the CPU time was ≈ 200 shorter for our algorithm. This time ratio tends to increase further with N. This is because the computational time to calculate the long-range energy in our method, which is usually the most expensive part of the computation, scales with $O(N)$ and the Lekner summation scales with $O(N^2)$.[31] It is noteworthy that our method when calculating the total energy, which includes the short-range part, also scales with $O(N^2)$. However, the short-range contribution is expected to be dominant only when the number of particles is much bigger. Also, this could be further mitigated using meshing schemes to reduce computational complexity.[18] This speedup may allow the simulations of highly dense ionic liquids at constant potential, simulations which previously had prohibitive times

of execution. Merging this algorithm with other techniques, such as Parallel Tempering recipes, will allow investigations into new regimes of ionic liquids.

Ionic liquids are a new class of materials sometimes referred to as solvent-free electrolytes or room-temperature plasmas.[10,24,26,30,44] This is because, even without a solvent, the charged molecules are in the liquid state at room temperature. Furthermore, their properties are highly tunable by engineering the molecules that will be synthesized. Then, for example, the dielectric constant or the size of the molecules can be modified by different synthesis techniques. They usually have lower dielectric constants than water and have bigger packing fractions, though this also can vary substantially.[44]

Following the literature, we define the volume fraction as the total volume occupied by the molecules divided by the volume of the simulation box, $\rho_v = \sum_i v_i/V$, where v_i is the volume of the molecules. We model the ionic liquid as hard spheres with 0.8 nm of diameter and volume fraction $\rho_v = 1/3$. To achieve the bulk regime in between the plates, we set them apart at distance $L = 24$ nm. We use the same number of k-vectors, MC steps, and L_d as in previous sections.

In a work by Kornyshev et al.,[43] it was shown that, depending on the applied voltage on a confined ionic liquid, the double layer can present two distinct behaviors: crowding and overscreening. In the crowding phenomenon, there are not enough ions to neutralize the plate within just one layer; hence, two layers are necessary, crowding the plate. Overscreening is characterized by the fact that one layer of ions has more surface charge density than the plate, therefore attracting a second layer of atoms with the opposite charge. In Figure 3a, we show that by tuning the Bjerrum length, that is, increasing the temperature or dielectric constant, one can have the two behaviors at the same potential. This is because, in such a highly interacting system, the average charge density on the plates does not depend only on the externally applied potential but also on the "internal" parameters of the system. In Figure 3b, we switch between double layers by the potential, as usual. We note, however, a "flat" portion of neutral charge between the first and the second layer of charge. This is probably because of the strong steric interactions present in ionic liquids. We hope that our results serve as benchmarks to complex liquid theories that aim to study such defying systems.

VI. CONCLUSIONS

We have presented a new Monte Carlo method to rapidly simulate ionic liquids in slab geometry at the constant potential ensemble. Merging two previous methods,[37,38] we retained the advantages of both of them. This is mainly because we avoided complex summations over modified spherical Bessel functions, computing just simple exponential series in the reciprocal space. Furthermore, we have shown equivalence between the method of constant surface charge and the method of constant potential. In addition, to lay our algorithm on solid grounds, we compared it with a Poisson–Boltzmann theory, achieving perfect consistency in the weak coupling limit. Finally, we studied room-temperature ionic liquids and showed that the alternation between crowding and overscreening can be controlled by the Bjerrum length alone, that is, by varying $k_B T$ or the dielectric constant of the liquid one can switch between behaviors. Our method has a major advantage that it can replace the KA algorithm by just changing the ionic–ionic interaction.

With this new method, it is easy and less error-prone to calculate the differential capacitance of ionic liquids by simply computing the dispersion of the surface charge density. With fast enough simulations, one can study how specific parameters modify the shape of the capacitance curve. That is, with the algorithm presented in this article, a new and systematic study of capacitance curves of ionic liquids at constant potential is possible. This is the subject of our future work.

■ AUTHOR INFORMATION

Corresponding Author

Matheus Girotto − *Instituto de Fisica, Universidade de Sao Paulo, 05508-090 Sao Paulo, SP, Brazil;* Email: matheus.girotto@usp.br.

Author

Adriano Mesquita Alencar − *Instituto de Fisica, Universidade de Sao Paulo, 05508-090 Sao Paulo, SP, Brazil;* ⓘ orcid.org/0000-0001-9324-2698

Complete contact information is available at:
https://pubs.acs.org/10.1021/acs.jpcb.0c03510

Notes

The authors declare no competing financial interest.

■ REFERENCES

(1) dos Santos, A. P.; Levin, Y. Electrolytes between Dielectric Charged Surfaces: Simulations and Theory. *J. Chem. Phys.* **2015**, *142*, No. 194104.

(2) Colla, T.; Girotto, M.; dos Santos, A. P.; Levin, Y. Charge Neutrality Breakdown in Confined Aqueous Electrolytes: Theory and Simulation. *J. Chem. Phys.* **2016**, *145*, No. 094704.

(3) Jing, Y.; Jadhao, V.; Zwanikken, J.; de La Cruz, M. O. Ionic Structure in Liquids Confined by Dielectric Surfaces. *J. Chem. Phys.* **2015**, *143*, No. 194508.

(4) Guerrero-García, G. I.; González-Tovar, E.; Chávez-Páez, M.; Kłos, J.; Lamperski, S. Quantifying The Thickness of The Electrical Double Layer Neutralizing a Planar Electrode: The Capacitive Compactness. *Phys. Chem. Chem. Phys.* **2018**, *20*, 262−275.

(5) dos Santos, A. P.; Girotto, M.; Levin, Y. Simulations of Polyelectrolyte Adsorption to a Dielectric Like-Charged Surfaces. *J. Phys. Chem. B* **2016**, *120*, 10387−10393.

(6) Nguyen, T.; Li, H.; Bagchi, D.; Solis, F. J.; de la Cruz, M. O. Incorporating Surface Polarization Effects into Large-Scale Coarse-Grained Molecular Dynamics Simulation. *Comput. Phys. Commun.* **2019**, *241*, 80−91.

(7) Girotto, M.; Colla, T.; dos Santos, A. P.; Levin, Y. Lattice Model of an Ionic Liquid at an Electrified Interface. *J. Phys. Chem. B* **2017**, *121*, 6408−6415.

(8) Limmer, D. T.; Merlet, C.; Salanne, M.; Chandler, D.; Madden, P. A.; van Roij, R.; Rotenberg, B. Charge Fluctuations in Nanoscale Capacitors. *Phys. Rev. Lett.* **2013**, *111*, No. 106102.

(9) Jiang, D. E.; Wu, J. Z. Microscopic Insights into The Electrochemical Behavior of Nonaqueous Electrolytes in Electric Double-Layer Capacitors. *J. Phys. Chem. Lett.* **2013**, *4*, 1260−1267.

(10) Merlet, C.; Limmer, D. T.; Salanne, M.; van Roij, R.; Madden, P. A.; Chandler, D.; Rotenberg, B. The Electric Double Layer Has a Life of Its Own. *J. Phys. Chem. C* **2014**, *118*, 18291−18298.

(11) Reed, S. K.; Lanning, O. J.; Madden, P. A. Electrochemical Interface Between an Ionic Liquid and a Model Metallic Electrode. *J. Chem. Phys.* **2007**, *126*, No. 084704.

(12) Monroe, C. W.; Daikhin, L. I.; Urbakh, M.; Kornyshev, A. A. Principles of Electrowetting with Two Immiscible Electrolytic Solutions. *J. Phys.: Condens. Matter* **2006**, *18*, 2837−2869.

(13) Monroe, C. W.; Daikhin, L. I.; Urbakh, M.; Kornyshev, A. A. Electrowetting with Electrolytes. *Phys. Rev. Lett.* **2006**, *97*, No. 136102.

(14) Frekel, D.; Smit, B. *Understanding Molecular Simulation*, 2nd ed.; Academic Press: San Diego, CA, 2002.

(15) Ewald, P. P. Die Berechnung optischer und elektrostatischer Gitterpotentiale. *Ann. Phys.* **1921**, *369*, 253−287.

(16) Darden, T.; York, D.; Pedersen, L. Particle Mesh Ewald: An Nlog(N) Method for Ewald Sums in Large Systems. *J. Chem. Phys.* **1993**, *98*, 10089−10092.

(17) Essmann, U.; Perera, L.; Berkowitz, M. L.; Darden, T.; Lee, H.; Pedersen, L. G. A Smooth Particle Mesh Ewald Method. *J. Chem. Phys.* **1995**, *103*, 8577−8593.

(18) Deserno, M.; Holm, C. How to Mesh Up Ewald Sums. I. A Theoretical and Numerical Comparison of Various Particle Mesh Routines. *J. Chem. Phys.* **1998**, *109*, 7678−7693.

(19) Deserno, M.; Holm, C. How to Mesh Up Ewald Sums. II. An Accurate Error Estimate for The Particle−Particle−Particle-Mesh Algorithm. *J. Chem. Phys.* **1998**, *109*, 7694−7701.

(20) Toukmaji, A. Y.; Board, J. A. Ewald Summation Techniques in Perspective: A Survey. *Comput. Phys. Commun.* **1996**, *95*, 73−92.

(21) Nymand, T. M.; Linse, P. Ewald Summation and Reaction Field Methods for Potentials with Atomic Charges, Dipoles, and Polarizabilities. *J. Chem. Phys.* **2000**, *112*, 6152−6160.

(22) Rhee, Y. J.; Halley, J. W.; Hautman, J.; Rahman, A. Ewald Methods in Molecular Dynamics for Systems of Finite Extent in One of Three Dimensions. *Phys. Rev. B* **1989**, *40*, No. 36.

(23) Harris, F. E. Ewald Summations in Systems with Two-Dimensional Periodicity. *Int. J. Quantum Chem.* **1998**, *68*, 385−404.

(24) Simon, P.; Gogotsi, Y. Materials for Electrochemical Capacitors. *Nat. Mater.* **2008**, *7*, 845−854.

(25) Armand, M.; Endres, F.; MacFarlane, D. R.; Ohno, H.; Scrosati, B. Ionic-liquid Materials for The Electrochemical Challenges of The Future. *Nat. Mater.* **2009**, *8*, 621−629.

(26) Wishart, J. Energy Applications of Ionic Liquids. *Energy Environ. Sci.* **2009**, *2*, 956−961.

(27) Chmiola, J.; Largeot, C.; Taberna, P. L.; Simon, P.; Gogotsi, Y. Monolithic Carbide-Derived Carbon Films for Micro-Supercapacitors. *Science* **2010**, *328*, 480−483.

(28) Liu, Y.; Lu, C.; Twigg, S.; Ghaffari, M.; Lin, J.; Winograd, N.; Zhang, Q. M. Direct Observation of Ion Distributions near Electrodes in Ionic Polymer Actuators Containing Ionic Liquids. *Sci. Rep.* **2013**, *3*, No. 973.

(29) Girotto, M.; dos Santos, A. P.; Levin, Y. Simulations of Ionic Liquids Confined by Metal Electrodes Using Periodic Green Functions. *J. Chem. Phys.* **2017**, *147*, No. 074109.

(30) Girotto, M.; Malossi, R. M.; dos Santos, A. P.; Levin, Y. Lattice model of ionic liquid confined by metal electrodes. *J. Chem. Phys.* **2018**, *148*, No. 193829.

(31) Lekner, J. Summation of Coulomb Fields in Computer-Simulated Disordered Systems. *Physica A* **1991**, *176*, 485−498.

(32) Arnold, A.; de Joannis, J.; Holm, C. Electrostatics in Periodic Slab Geometries. I. *J. Chem. Phys.* **2002**, *117*, 2496−2502.

(33) de Joannis, J.; Arnold, A.; Holm, C. Electrostatics in Periodic Slab Geometries. II. *J. Chem. Phys.* **2002**, *117*, 2503−2512.

(34) Kawata, M.; Mikami, M. Rapid Calculation of Two-Dimensional Ewald Summation. *Chem. Phys. Lett.* **2001**, *340*, 157−164.

(35) Mazars, M. Lekner Summations. *J. Chem. Phys.* **2001**, *115*, 2955−2965.

(36) Yeh, I. C.; Berkowitz, M. L. Ewald Summation for Systems with Slab Geometry. *J. Chem. Phys.* **1999**, *111*, 3155−3162.

(37) dos Santos, A. P.; Girotto, M.; Levin, Y. Simulations of Coulomb Systems with Slab Geometry Using an Efficient 3D Ewald Summation Method. *J. Chem. Phys.* **2016**, *144*, No. 144103.

(38) Kiyohara, K.; Asaka, K. Monte Carlo Simulation of Electrolytes in The Constant Voltage Ensemble. *J. Chem. Phys.* **2007**, *126*, No. 214704.

(39) Stenhammar, J.; Trulsson, M.; Linse, P. Some Comments and Corrections Regarding The Calculation of Electrostatic Potential Derivatives Using The Ewald Summation Technique. *J. Chem. Phys.* **2011**, *134*, No. 224104.

(40) Laino, T.; Hutter, J. Notes on "Ewald summation of electrostatic multipole interactions up to quadrupolar level" [J. Chem. Phys. 119, 7471 (2003)]. *J. Chem. Phys.* **2008**, *129*, No. 074102.

(41) Levin, Y. Electrostatic Correlations: from Plasma to Biology. *Rep. Prog. Phys.* **2002**, *65*, 1577−1632.

(42) Kornyshev, A. A. Double-Layer in Ionic Liquids: Paradigm Chance. *J. Phys. Chem. B* **2007**, *111*, 5545−5557.

(43) Bazant, M. Z.; Storey, B. D.; Kornyshev, A. A. Double Layer in Ionic Liquids: Overscreening versus Crowding. *Phys. Rev. Lett.* **2001**, *106*, No. 046102.

(44) Fedorov, M. V.; Kornyshev, A. A. Ionic Liquids at Electrified Interfaces. *Chem. Rev.* **2014**, *114*, 2978−3036.